SOME DYNAMICAL PROPERTIES OF VERY STRONG DOUBLE LAYERS IN A TRIPLE PLASMA DEVICE

T. Carpenter
Department of Physics
University of Iowa
Iowa City, Iowa 52242, U.S.A.

and

S. Torvén
Department of Plasma Physics, Royal Inst. of Technology, Stockholm, Sweden

I. INTRODUCTION

Since double layers observed in space and in simulations are rarely if every static, considerable attention has been given to studies of motions of double layers in the laboratory. Extensive reviews have recently been published of the dynamical properties of very strong double layers ($eV/kT_e \sim 1000$) in a Q machine (Sato et al., 1983; Iizuka et al., 1983) and strong double layers ($eV/kT_e \sim 10$) in a triple plasma device (Hershkowitz, 1985). In both cases the double layers were essentially planar. We report here on some of the dynamical properties of very strong double layers ($eV/kT_e \sim 200$) seen in a differentially pumped triple plasma device (Torvén, 1982). These double layers are V-shaped. In particular, we discuss the following findings: (1) Disruptions in the double layer potential and in the plasma current occur when an inductance is placed in series with the bias supply between the sources in the external circuit. These disruptions, which can be highly periodic, are the result of a negative resistance region that occurs in the I-V characteristic of the device. This negative resistance is due to a potential minimum which occurs in the low potential region of the double layer, and this minimum can be explained as the self-consistent potential required to maintain charge neutrality in this region. (2) When reactances in the circuit are minimized, the double layer exhibits a jitter motion in position approximately equal to the double layer thickness. The speed of the motion is approximately constant and is on the order of 2 times the ion-sound speed. The shape of the double layer does not change significantly during this motion. (3) When the bias between the sources is rapidly turned on, the initial phase in the double layer formation is the occurrence of a constant electric field (uniform slope of the potential) for the first few microseconds. The potential then steepens in the region where the double layer will eventually be formed and flattens in regions above and below this. The double layer is completely formed after about 100 microseconds and then engages in the jitter motion discussed above.

In the following we discuss first the apparatus used in all of the work and then consider each of the three phenomena mentioned above. In the first case it is believed that the phenomenon is rather completely understood and the situation is discussed at some length. The same cannot be said for the last two cases and limited discussion is included. However, these two phenomena have characteristics which differ qualitatively from what is seen in Q machines and these differences are identified.

II. EXPERIMENTAL DETAILS

The experiment was performed in a triple plasma device (Torvén, 1982) consisting of a central chamber with coaxial plasma sources located on either side as shown in Figure 1. Plasma was produced in the sources by discharges in argon between heated tungsten filaments and the source chamber walls. The electrodes B1 and B2 can also be used as anodes; but, for the present investigation, they were left floating. They, therefore, acquired potentials approximately equal to the respective filament potentials. The sources were independent in the sense that

discharge voltages and currents and gas flow rates could be varied independently in either source with unmeasurably small effects on the plasma parameters in the other source. The potential between the anodes of the two sources was determined by U_0, which was also taken as the difference in the plasma potentials in the sources. This assumption was tested several times during the course of the experiments using collecting probes in the sources to measure the potentials there and was found to be satisfied within the accuracy with which the potentials could be determined from the probe characteristics, or about ± 0.5 volt, over a variation of U_0 by more than 200 volts. Plasma diffused into the central chamber from the sources through apertures A1 and A2 in the end plates of the central chamber. These apertures determined the diameter of the plasma column (3.0 cm) which was radially confined by a homogeneous magnetic field of up to 20 mT. Because of the small diameter of the apertures compared to the diffusion pump (25 cm), it was possible to maintain sufficient pressure in the sources for their proper operation (10 to 100 mPa) while restricting the pressure in the central chamber to about 1 mPa, thereby minimizing the importance of ionizing processes in the chamber. It is this property that allows the production of very strong double layers (potential drops up to 3 kV) in this device (Torvén, 1982).

Electric potentials were measured with electron emitting probes which could be moved both radially and axially with electric motors. For low frequency measurements (from d.c. up to about 10 kHz), the probes were operated essentially at their floating potential, which was measured using 100 mohm frequency-compensated voltage dividers. For a.c. signals which are not too large (cf. Torvén et al., 1985), the frequency response of the probe is determined by the product of the dynamic resistance of the plasma near the floating potential and the distributed capacitance of the probe and its heating circuit. This capacitance (about 100 pf) is dominated by the capacitance to ground of the feed wires to the movable probe inside the vacuum chamber. The dynamic resistance of the plasma, defined as the reciprocal of the slope of the probe characteristic, depends on the plasma density and the probe wire temperature. For the present experiment it was on the order of 10 kohm.

III. DISRUPTIONS WITH AN INDUCTIVE EXTERNAL CIRCUIT

When an inductor of sufficient size is placed in series with the bias source U_0, it is observed that periodic disruptions of the plasma current and of the double layer potential occur. These disruptions have been previously reported in detail (Torvén et al., 1985) and we review here only those aspects pertinent to the present work.

Figure 2 shows an example of the disruptions when the inductance was 0.1 Hy. The top oscilloscope trace shows that the potential measured on the positive source varied from zero to 400 volts. For these runs U_0 was 100 volts so there was a 300-volt inductive overvoltage. This overvoltage was given exactly by L dI/dt, where I is the current flowing through the inductor. This current is shown by the bottom trace in Figure 2. The other traces are of potentials measured by probes at fixed positions in the plasma and show that the potential drop does occur over a limited spatial region, that is, in a double layer.

The disruptions are thus seen to be completely explained in terms of variations in the plasma current. The plasma current, in turn, is controlled by the potential structure between the two sources. Figure 3 shows the potential measured in the low potential region for various times during the disruption cycle. There is clearly qualitative agreement between the minimum value of the potential, which should be the only feature of the potential structure that influences the plasma current, and the plasma current. To test the quantitative sufficiency of this mechanism, a series of experiments were performed with the inductance removed and with U_0 varied slowly over the voltage range of interest. Preliminary reports of these results have appeared (Carpenter and Torvén, 1984; Carpenter et al., 1984), and a detailed account will appear (Carpenter and Torvén, 1986), but we will review the pertinent results here.

To obtain I-V characteristics of the device, the potential U_0 between the sources was slowly varied, either by hand or by using a function generator to control the power supply with voltage-control programming, and the resulting plasma current measured using precision 1 ohm shunts. The data were taken using a calibrated X-Y plotter, or a calibrated two-parameter transient digitizer. The emitting probes were used to measure both axial and radial potential profiles for different values of U_0. An example of the axial potential structure observed between the sources is shown in Figure 4. For these data U_0 was 150 volts. A minimum in the potential is clearly seen at about 15 cm from the left aperture. That the minimum is in fact quite well defined is seen more clearly with the expanded scale. The magnitude of the minimum potential, V_m, was determined for values of U_0 between zero and 200 volts. For details of how this was accomplished see Carpenter and Torvén (1986). An example of such a measurement is shown in the lower half of Figure 5. The corresponding I-V characteristic is shown as the solid curve in the upper half of this figure.

The purpose of these measurements, as mentioned above, was to test whether or not the variations in V_m could quantitatively explain the variations in the plasma current. For purposes of this discussion, consider only the case where the right source is biased positive with respect to the left source. Plasma from both sources diffuses into the central chamber. Since a potential minimum exists between the sources, the ion flow will not be affected, but the electron current between the sources will be reduced because of reflection of electrons from both sources by an amount that depends only on the differences between the minimum potential V_m and the plasma potentials in the sources. These potential differences can be obtained from the data, and the I-V characteristics can accordingly be calculated if the electron distribution functions are known.

Assume that the plasmas in the sources are Maxwellian with temperatures T_p and T_n and densities n_p and n_n, where the subscripts p and n refer to the positive and negative sources, respectively. These symbols refer to the electrons only. (Ion currents can be easily included, but they contribute much less than 1 percent of the total current and so are ignored in order to simplify the notation.) Then the distribution function at a point where the potential is V(x) is generally given by

$$f(x,v) = n_0 \left(\frac{2m}{\pi kT}\right)^{1/2} \exp\left[-\frac{mv^2}{2kT} - \frac{e(V_0 - V(x))}{kT}\right] \qquad \text{for} \qquad a < v < \infty$$

$$= 0 \quad \text{for velocities outside this range} \quad . \tag{1}$$

Here n_0 is the plasma density at a point where the potential is V_0, e is the magnitude of the electronic charge, m is the electron mass, and k is the Boltzman constant. The lower velocity limit a is negative for points between the source and the minimum, since reflected electrons exist in this region, and positive for points beyond the minimum. It is exactly zero at the minimum, so the lower limit is the velocity such that the energy, which is constant, is just equal to V_m. Thus,

$$a = \pm \left\{\left(\frac{2e}{m_e}\right)\left[V(x) - V_m\right]\right\}^{1/2} \quad . \tag{2}$$

The current is of course independent of the point x where it is evaluated. However, it is convenient to evaluate the contributions to the total current from each source at the position of the potential minimum, since at this point the distribution functions take on their simplest forms. The result is

$$I = Ae \left\{\left(\frac{2k}{\pi m_e}\right)^{1/2}\left[n_n T_{en}^{1/2} \exp\left(-\frac{V_n - V_m}{kT_{en}}\right) - n_p T_{ep}^{1/2} \exp\left(-\frac{V_p - V_m}{kT_{ep}}\right)\right]\right.$$

$$\left. + \left(\frac{2k}{\pi m_i}\right)^{1/2}\left[n_p T_{ip}^{1/2} \exp\left(-\frac{V_p - V_n}{kT_{in}}\right)\right]\right\} \quad . \tag{3}$$

Here V_p and V_n are the plasma potentials in the sources and the other quantities have been defined previously. As the applied voltage U_0 is increased, the current increases at first because of the decrease in the magnitude of the second term. That is, V_p approximately follows U_0 and V_n stays approximately at ground. After U_0 increases to several times kT_p, the second term will become negligible, and further changes in I can only occur if V_m changes relative to V_n.

In order to test the sufficiency of this picture, we have used the measured variation of V_m with U_0 and determined the values of the temperatures and densities that best fit the data with equation (3). That is, the value of V_m observed at $U_0 = V_p - V_n$ is used in equation (3) to calculate I_{fit} and the results compared with the corresponding observed currents I_{exp}. The parameters in equation (3) are varied in order to minimize the sum

$$\psi = \sum (I_{exp} - I_{fit})^2 \quad . \tag{4}$$

The result of a typical fit is shown by the dashed line in the upper part of Figure 5. The main features of the data are certainly rather well explained. However, the temperatures that give acceptable fits are larger than those observed with probes in the sources. For example, the temperatures that give the fit shown in Figure 5 are 12.3 eV for the left source and 21.5 eV for the right source. Measured values for the temperatures were about 8 eV in both sources. However, the probe characteristics showed high energy tails of the type usually seen in discharge sources corresponding to a significant population of ionizing electrons. If distributions corresponding to such electrons were included in the model, the best-fit temperatures of the Maxwellian populations would certainly be reduced. However, the number of parameters to be fit would be doubled, thereby reducing the significance of the small improvement in the fit that might be expected. It is felt that the appropriateness of the model has been adequately demonstrated without this refinement. Data were taken and fits performed in the manner described for 12 different combinations of source parameters, such that the plasma density in both sources varied by an order of magnitude. No unusual characteristics were observed and the fits obtained were in all cases comparable to that described above.

The model can also be used to provide some insight into the role of the potential minimum and its behavior. The basic feature of the region of space below the double layer is its charge neutrality. That is, even though there are variations in the potential here, they occur over many hundreds, even thousands, of Debye lengths, so the departure of the ratio of electron-to-ion densities from unity is expected to be vanishingly small. Therefore, since the electron and ion charge densities depend in different ways on the voltage applied between the sources, some self-adjusting potential is needed between the sources in order to keep the region quasineutral. Mathematically, the requirement that the net charge density at the minimum be zero will insure quasineutrality over a broad region near this point. The electron densities were obtained by integrating the distribution functions given in equation (1) over the appropriate velocity intervals. The ion densities were obtained in a similar way. The form of the distribution functions was the same, but the velocity intervals were different since the ions were accelerated from the sources. The equation giving zero net charge at the minimum is

$$\begin{aligned} n_{ep} \exp\left(-\frac{V_p - V_m}{T_{ep}}\right) + n_{en} \exp\left(-\frac{V_n - V_m}{T_{en}}\right) &= n_{if} \exp\left(\frac{V_p - V_m}{T_{ip}}\right) \\ \times \left[1 - \operatorname{erf}\left(\sqrt{\frac{V_p - V_m}{T_{ip}}}\right)\right] + n_{in} \exp\left(\frac{V_n - V_m}{T_{in}}\right) \\ \times \left[1 + \operatorname{erf}\left(\sqrt{\frac{V_p - V_m}{T_{in}}}\right) - 2 \operatorname{erf}\left(\sqrt{\frac{V_n - V_m}{T_{in}}}\right)\right] \quad , \end{aligned} \tag{5}$$

where the new subscripts i and e refer to the ions and electrons. This equation was solved by simply stepping V_m, in successively smaller steps each time zero was crossed, until the step size was smaller than the accuracy desired. The results are sensitive to the ion temperatures, about which we have little experimental information. Examples showing how V_m varies as $U_0 = V_p - V_n$ is changed are shown in Figure 6 for three different sets of ion temperatures. The plasma parameters used were typical of those observed experimentally in the two sources. It seems clear that a rather good fit to the experimental curve of V_m versus U_0 could be obtained by adjusting the ion parameters, with possibly some small adjustment of the electron parameters, but in view of the number of parameters involved and the fact that the charge exchange ions have been neglected, such an effort hardly appears justified. However, the agreement with the data of the trends shown in Figure 6 provides some confidence in the following explanation: As U_0 is first increased, the biggest change is the reduction in the number of electrons reaching the minimum region from the positive source. To compensate, the minimum becomes less negative so more electrons from the negative source are admitted. This continues until all electrons from the positive source are reflected. Competing with this effect is the reduction of ion density from the positive source due to increasing ion velocity as U_0 increases and when the electrons are eliminated, this effect becomes dominant. Thus, the minimum increases in depth to reduce the flow of electrons from the negative source. It is exactly this last process that gives rise to the negative resistance region according to this model.

The main features of the variation of V_m with U_0 are obviously rather well explained by these considerations, at least for cases where U_0 varies slowly with time. Thus, the negative-resistance region in the I-V characteristic is explained, and it can be said that the low frequency disruptions are understood. It should be emphasized that in order to observe disruptions of low enough frequency that this explanation applies without modification, additional lumped capacitance must be added in parallel with the distributed capacitance between the sources (Carpenter et al., 1984). At higher frequencies ion-transit times become significant and there is some delay in the charge neutrality condition that can be expected to affect V_m. Although these effects have not been included, it seems clear that careful consideration of the potential structure in the low potential region must be included in any complete theory of double layers.

IV. JITTER MOTION

When the potential indicated by the emissive probe is monitored by a device capable of following high frequency variations, such as an oscilloscope, it is observed that the signal fluctuates wildly when the probe is in the vicinity of the double layer. Observations as the probe moves through the double layer lead quickly to the conclusion that the fluctuations are due to the random motion of the entire potential structure around its equilibrium position. The effect is shown in Figure 7. These data were recorded by plotting single sweeps obtained with a transient digitizer on the same graph. Also shown is an overlay of the double layer obtained with an X-Y plotter during this run. The sweeps were obtained with the probe fixed at the three positions marked A, B, and C on the double layer. For all three sets of sweeps, horizontal lines are shown that correspond to the variation in potential which results when the double layer makes an excursion with a total extent of 1.2 cm centered at each of the three points. Clearly the various amplitudes of the fluctuations which are observed as the probe moves through the double layer are all explained by movements of the structure by a constant amount. Also evident in these data are regions where the potential changes with a constant slope for several microseconds. The velocity of the structure is apparently constant during these times. Since the double layer provides a convenient conversion factor — distance required for a given potential change — the velocity of the motion can be determined if we can determine the change in shape of the double layer (the calibration constant) as it undergoes its random motion.

The X-Y plotter provides a potential profile which is time-averaged over the rapid jitter motion. To obtain instantaneous profiles, a second stationary probe was mounted in the double layer slightly off-axis. The signal from

this probe provided a trigger which gated the output of the moving probe used to map the potential structure. The varying signal from the trigger probe corresponded to varying positions of the structure. Thus, different double layer positions could be selected by choosing different trigger levels. Data obtained with three different levels are shown in Figure 8. If any of the curves is displaced horizontally, it is seen to closely overlap the other two curves. We conclude that the double layer moves with little, if any, change in shape. Another interesting implication of this result should be mentioned. The fact that double layer shapes that have been previously reported are time averages has been invoked by some authors to explain the apparent broadness of laboratory double layers. However, the widths of the instantaneous profiles reported here, defined for example as the distance required for a change from 10 percent to 90 percent of the full height, are not significantly different from those obtained with an X-Y plotter. This is the expected result if the structure between the 10 percent and 90 percent points was a straight line, the velocity was constant, and the maximum excursion was equal to the double layer width, which seems to be approximately the case.

The data in Figure 7 indicate that motion toward the negative source, corresponding to an increasing potential, occurs with a higher velocity than motion toward the positive source. However, this apparent difference is entirely due to experimental effects associated with the distributed capacitance of the emissive probe to ground. This was first suspected when it was noticed that the apparent difference was reduced when the emissive probe was shunted with an external resistor. The distributed capacitance can easily be charged more positively by simply emitting electrons. However, to become more negative it must collect electrons and it has insufficient area to do this rapidly enough. Put another way, the time response of the probe is determined by its RC time constant, where C is the distributed capacitance and R is the dynamic resistance of the plasma, defined as the reciprocal of the slope of the probe's I-V characteristic. The distributed capacitance is on the order of 100 pF and the dynamic resistance of the probe normally is on the order of 10 kohms. Thus,RC is on the order of 1 microsecond and the probe can respond to changes on the order of 1 MHz. However, when the probe is collecting electron saturation current, which would happen if the plasma potential suddenly dropped, the dynamic resistance is on the order of a few megohms, giving RC on the order of a tenth of a millisecond.

In order to overcome this effect, a special emissive probe was constructed in which the heating circuit, which contributed almost all of the distributed capacitance, was mechanically disconnected from the potential measuring circuit during the measurement time. The distributed capacitance during the measuring time was reduced to 10 pF which gives an RC value of 10 microseconds even in the worse case. Some traces of the fluctuating potential taken with this probe are shown in Figure 9. There is still a slight difference between the maximum rates of increase and decrease, but it is small enough that it can be explained as a residual effect of the distributed capacitance of the probe. The details of this probe and a further discussion of the effect of distributed capacitance on probe measurements will appear elsewhere (Torvén, private communication, 1986).

The maximum rates of increase and decrease shown by overdrawn lines in Figure 8 are 36 and 24 volts per microsecond, respectively. The central portion of the double layer observed for this case had a slope of 50 volts per centimeter. Thus, the indicated velocities are 7.2 and 4.8 $\times$ 10^5 cm/s. As a comparison, the electron temperature observed for this run was 7 eV so the ion-acoustic speed was 4.1 $\times$ 10^5 cm/s.

Fluctuations are observed also in double layers formed in Q machines (Iizuka et al., 1983; Sato et al., 1981). In the case of double-ended operation, the mode most comparable to the triple plasma machine, nearly stationary double layers are observed. The fluctuation consists of a more or less periodic variation of the slope of the double layer with the knee at the high potential side remaining approximately fixed. Thus, the knee at the low potential side shows a sort of roughly periodic motion which has been termed a "foot-point oscillation."

V. INITIAL FORMATION

In order to study the initial formation of the double layer, U_0 was replaced by a transistor-switched power source capable of supplying 100 volts with a rise time on the order of 1 microsecond. Standard boxcar sampling techniques were then used to measure the potential structure at various times after the bias voltage was switched on. Typical results are shown in Figure 10. There is a small structure near the low potential source that seems to propagate toward the high potential source, but the striking feature of the potential structure is that at early times the slope is essentially a constant. As time progresses the slope steepens in the vicinity of the place where the double layer will eventually form while it flattens in regions above and below this. The structure is nearly formed after 50 microseconds and completely formed after 100 microseconds. If one wants to think of the low potential foot-point as propagating toward the high potential source, then its velocity of propagation is about 50 cm in say 100 microseconds or 5×10^5 cm/s, a speed which is somewhat supersonic and which seems to be typical of the propagation velocity of the double layers in this device.

The initial formation of double layers has also been studied in a double-ended Q machine (Iizuka et al., 1983). In this work it was observed that immediately following the application of the bias voltage the potential rose to the positive source potential over nearly all of the column, forming an ion-rich sheath near the cathode. This condition persisted for about 100 microseconds, after which the double layer detached itself from the cathode and propagated, as a completely formed structure, toward its final position. The velocity of propagation was approximately 3 times the ion-sound speed.

It has been suggested that the motion of laboratory double layers represents a sort of "hunting" for that position where the Langmuir criterion (the square of the electron-to-ion current ratio equals the ion-to-electron mass ratio) is satisfied (Iizuka et al., 1983; Torvén, 1982). The basis for this explanation is that the ion flux at the double layer should decrease as the length of the high potential region increases because of radial losses of ions along the part of the column at high potential. It should be expected, then, that the larger these losses are, the smaller should be the excursions from the equilibrium position. This may explain why the double layers seen with relatively weak magnetic fields are more stable than those seen in the Q machines. It may also explain the lack of stability of double layers seen in simulations where the use of periodic boundary conditions at the sides is equivalent to the total removal of radial ion losses. In order to investigate this question, a systematic investigation should be made of the motion of double layers as a function of the strength of the magnetic field and the planarity of the plasma column.

Acknowledgments. This work was performed at the Royal Institute of Technology in Stockholm. One of us (RTC) would like to thank Carl-Gunne Fälthammer for the stimulating working conditions that were provided and also the Swedish Natural Science Research Council and the Swedish Institute for support during the stay in Sweden.

REFERENCES

Carpenter, R. T., and S. Torvén, *Proc. Int. Conf. on Plas. Phys.*, Lausanne, P14-3, 1984.

Carpenter, R. T., S. Torvén and L. Lindberg, in *Second Symposium on Double Layers and Related Topics*, edited by R. Schrittwieser and G. Eder, p. 159, University of Innsbruck, 1984.

Carpenter, R. T., and S. Torvén, to be published, 1986.

Hershkowitz, N., *Space Sci. Rev., 41,* 351, (1985).

Izuka, S., P. Michelsen, J. Juul Rasmussen, R. Schrittwieser, R. Hatakeyama, K. Saeki, and N. Sato, Riso National Laboratory Report RISO-M-2414, 1983.

Sato, N., R. Hatakeyama, S. Iizuka, T. Mieno, K. Saeki, J. Juul Rasmussen, and P. Michelsen, *Phys. Rev. Lett., 46,* 1330 (1981).

Sato, N., R. Hatakeyama, S. Iizuka, T. Mieno, K. Saeki, J. Juul Rasmussen, P. Michelsen, and R. Schrittwieser, *J. Phys. Soc. Jpn., 52,* 875 (1983).

Torvén, S., *J. Phys. D., Appl. Phys., 15,* 1943 (1982).

Torvén, S., L. Lindberg, and R. T. Carpenter, *Plasma Phys., 27,* 143 (1985).

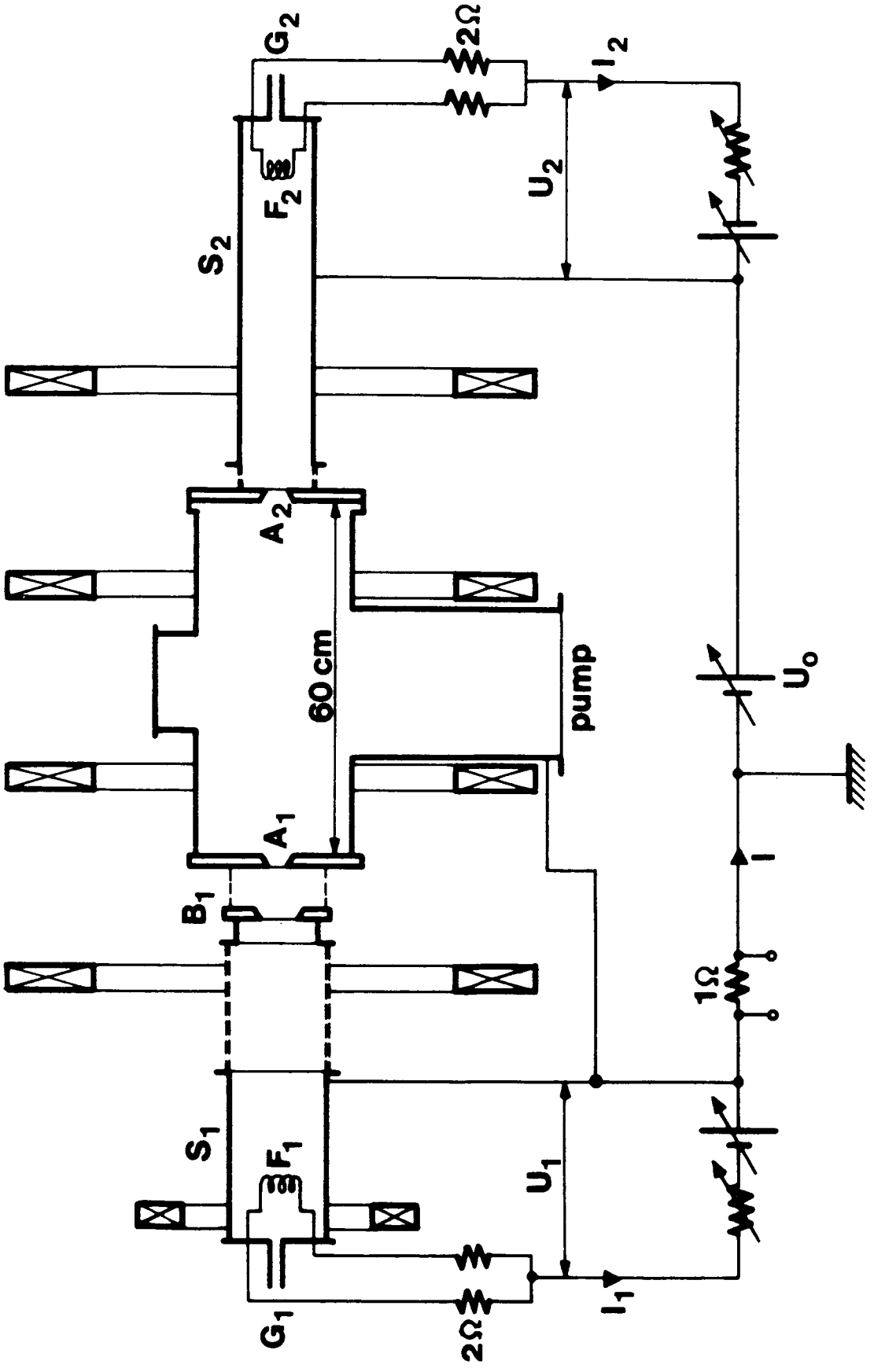

Figure 1. Schematic of the triple plasma machine.

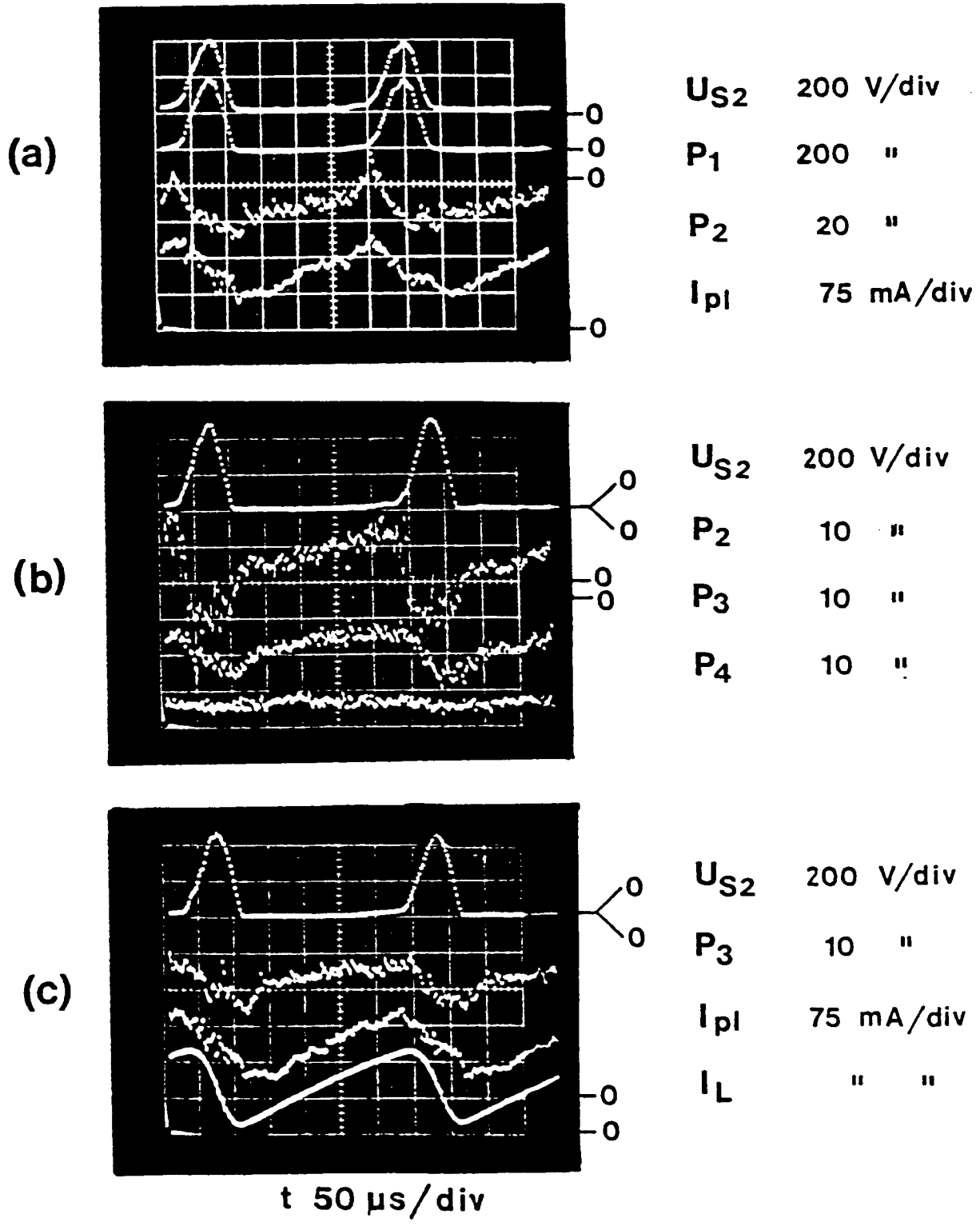

Figure 2. Oscilloscope traces during the disruptions. Probes P1, P2, P3, and P4 were located at 55, 45, 20 and 6 cm from aperture A1. The gain settings and zero levels are different for the various sweeps and are indicated to the right of each trace.

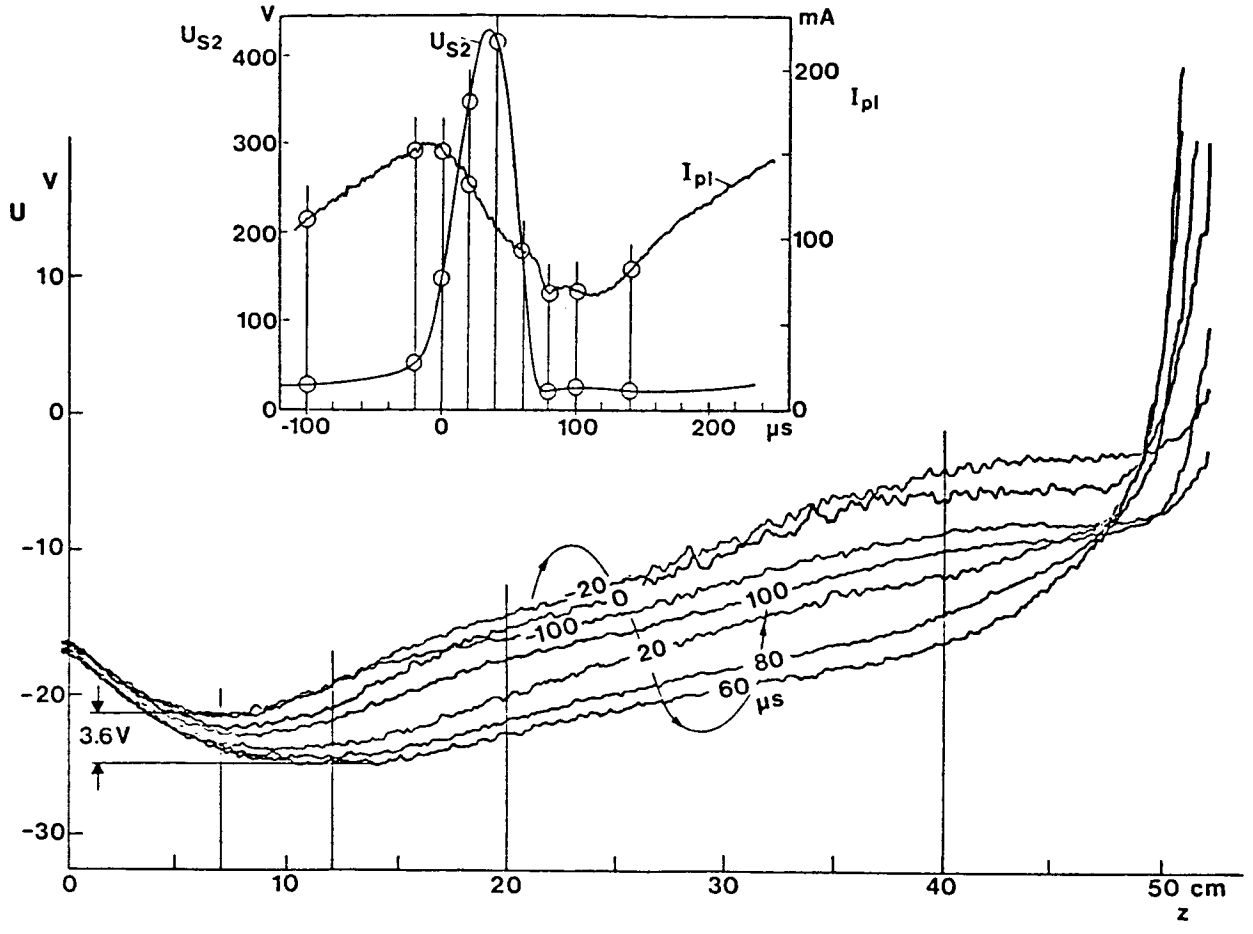

Figure 3. Potential structure in the low potential region sampled at various times, indicated by circles in the inset, during the disruption cycle. The serpentine line shows the timing sequence and the inset shows the time variation of the plasma current and the positive source potential.

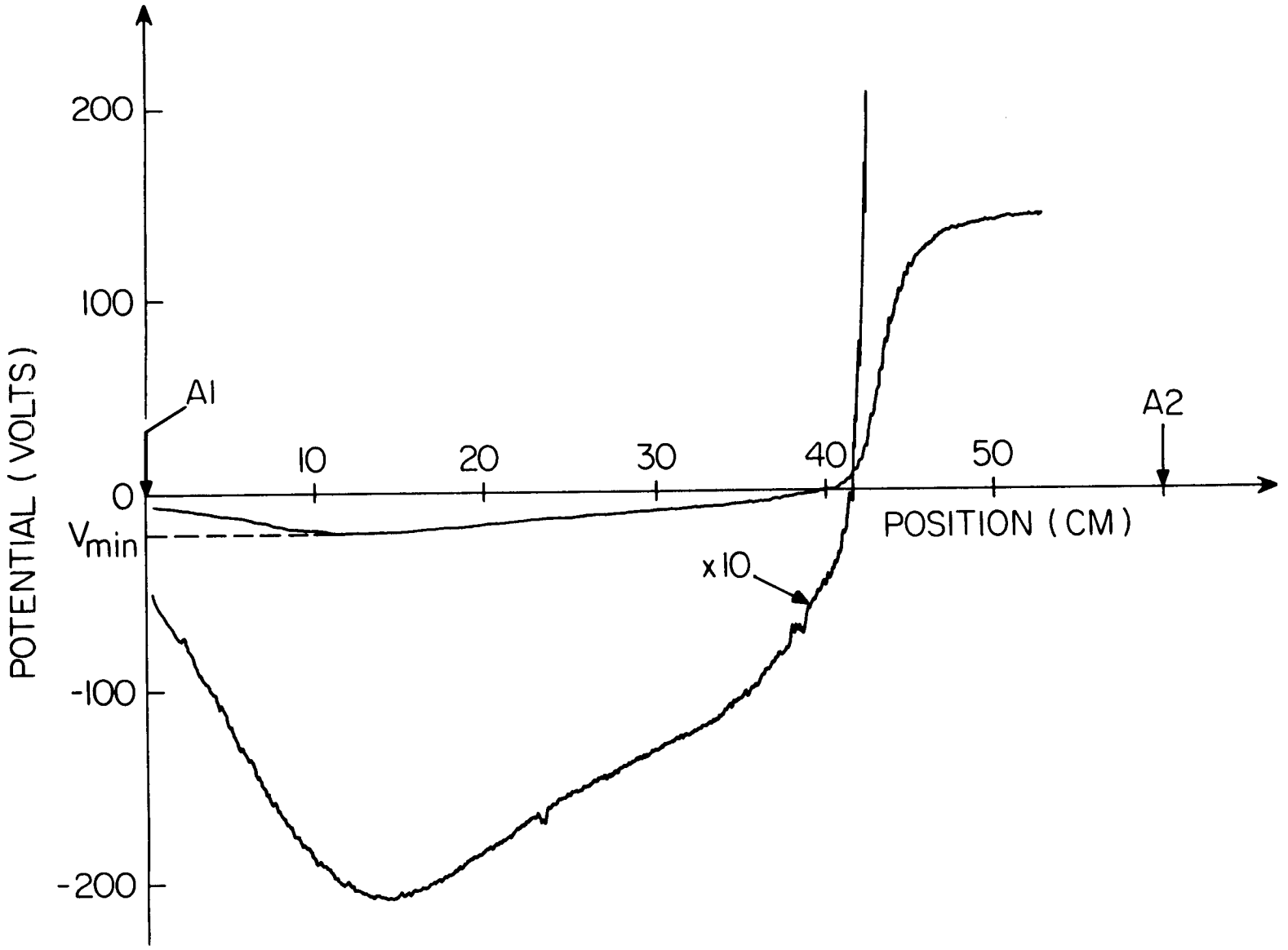

Figure 4. Steady state double layer showing the potential minimum in the low potential region.

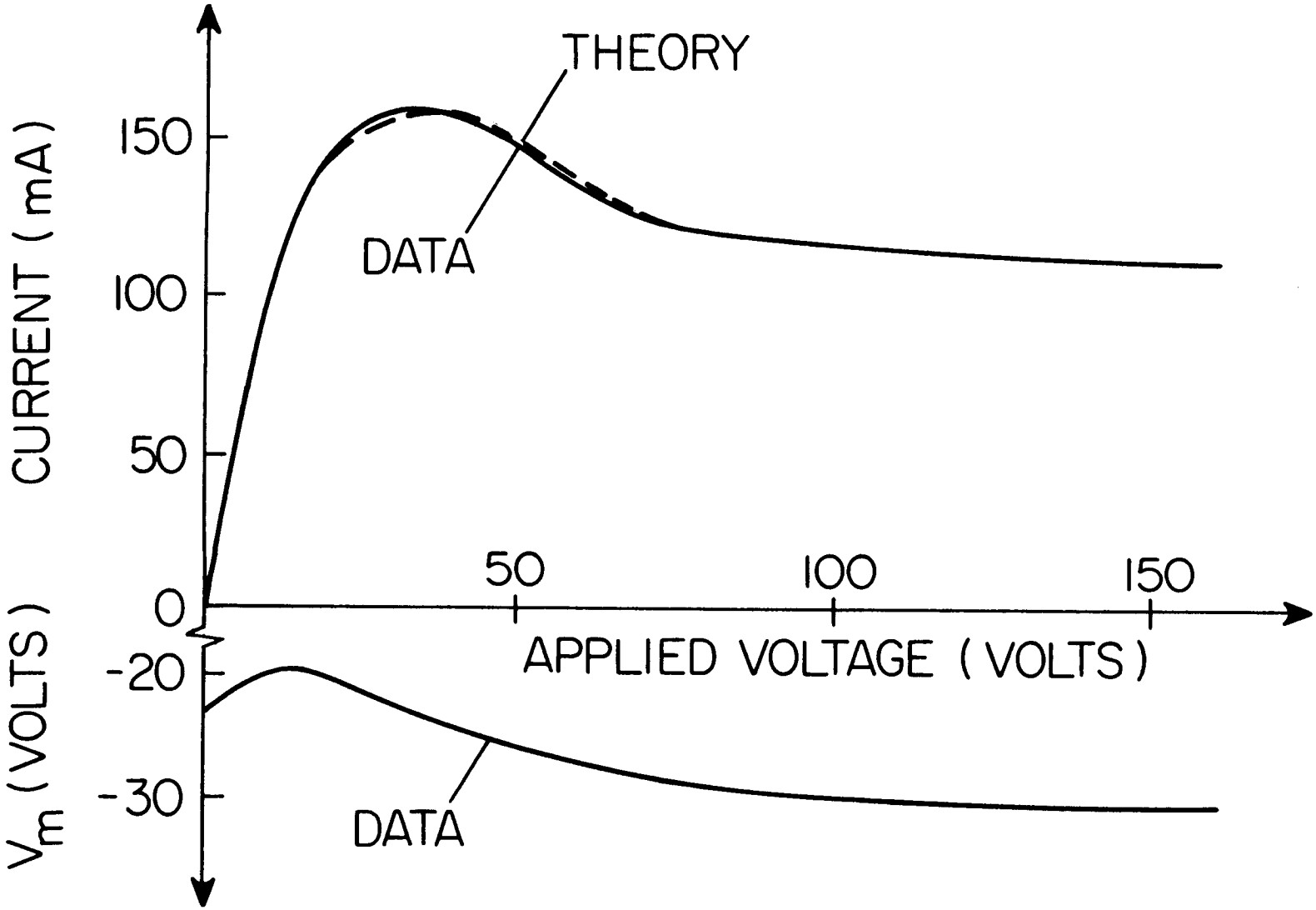

Figure 5. I-V characteristic for the double layer (upper curve) and the variation of the current-limiting minimum (lower curve). A fit to the I-V chracteristic, using the data in the lower curve and assuming Maxwellian distributions in the sources, is shown by the dashed curve.

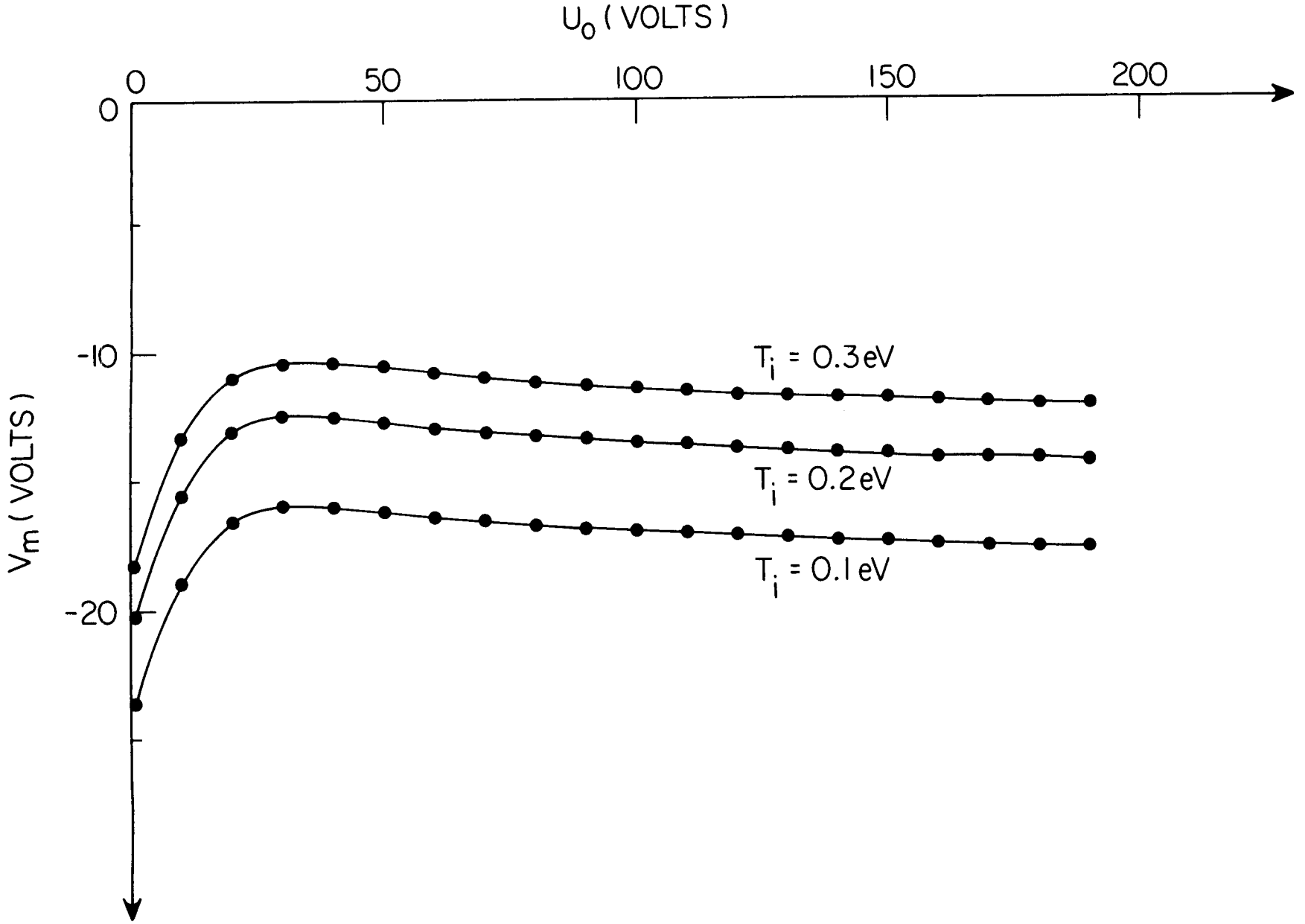

Figure 6. Examples of the calculated variation of the potential minimum V_m required to produce charge neutrality at the minimum. The ion temperatures were assumed to be the same in both sources.

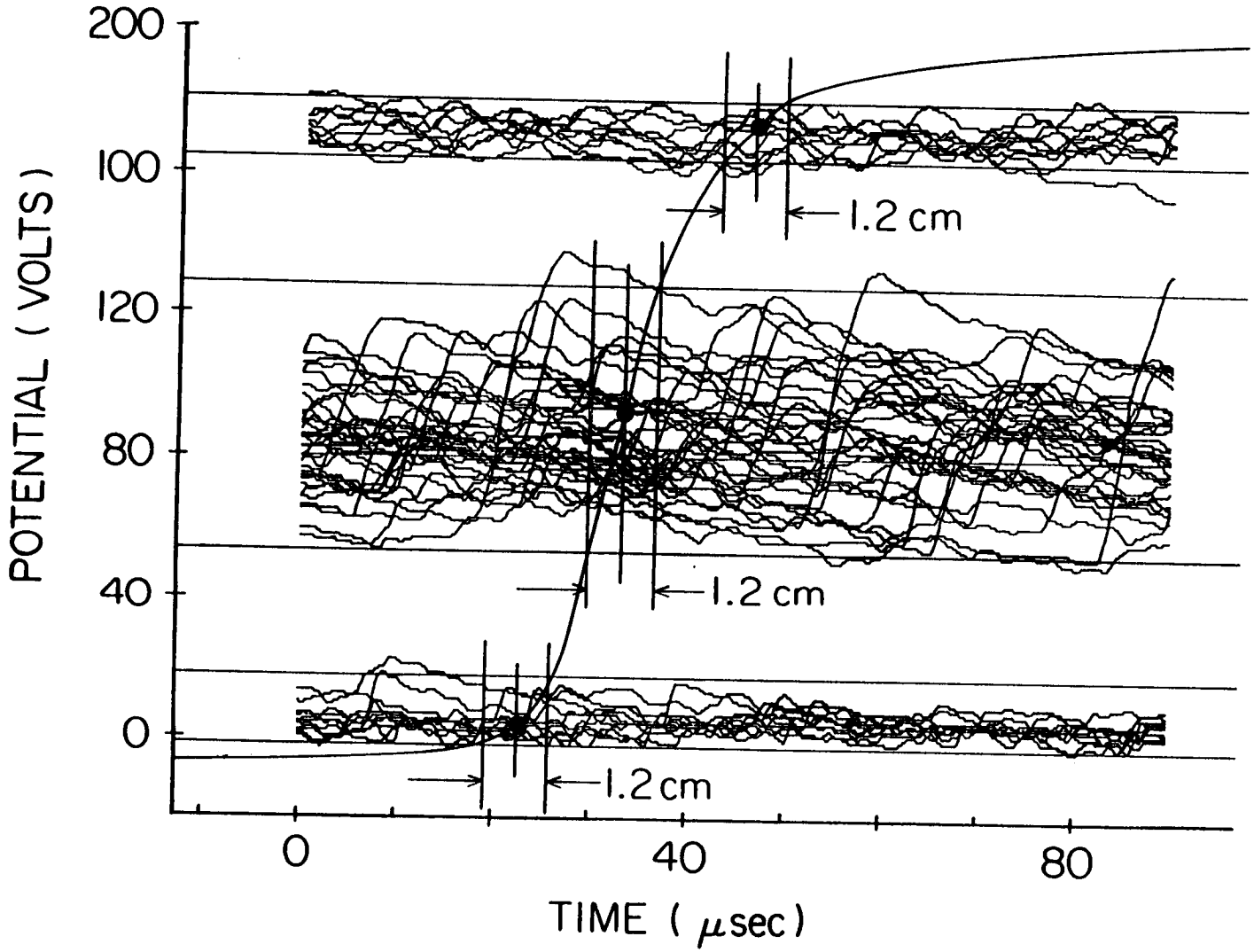

Figure 7. Oscilloscope traces, obtained with a digital transient recorder, of the potential indicated by an emissive probe when the probe was located at three different positions in the double layer. The positions chosen are shown on the overdrawn double layer which also shows potential variations corresponding to excursions in the double layer position by a total of 1.2 cm, centered at the indicated points.

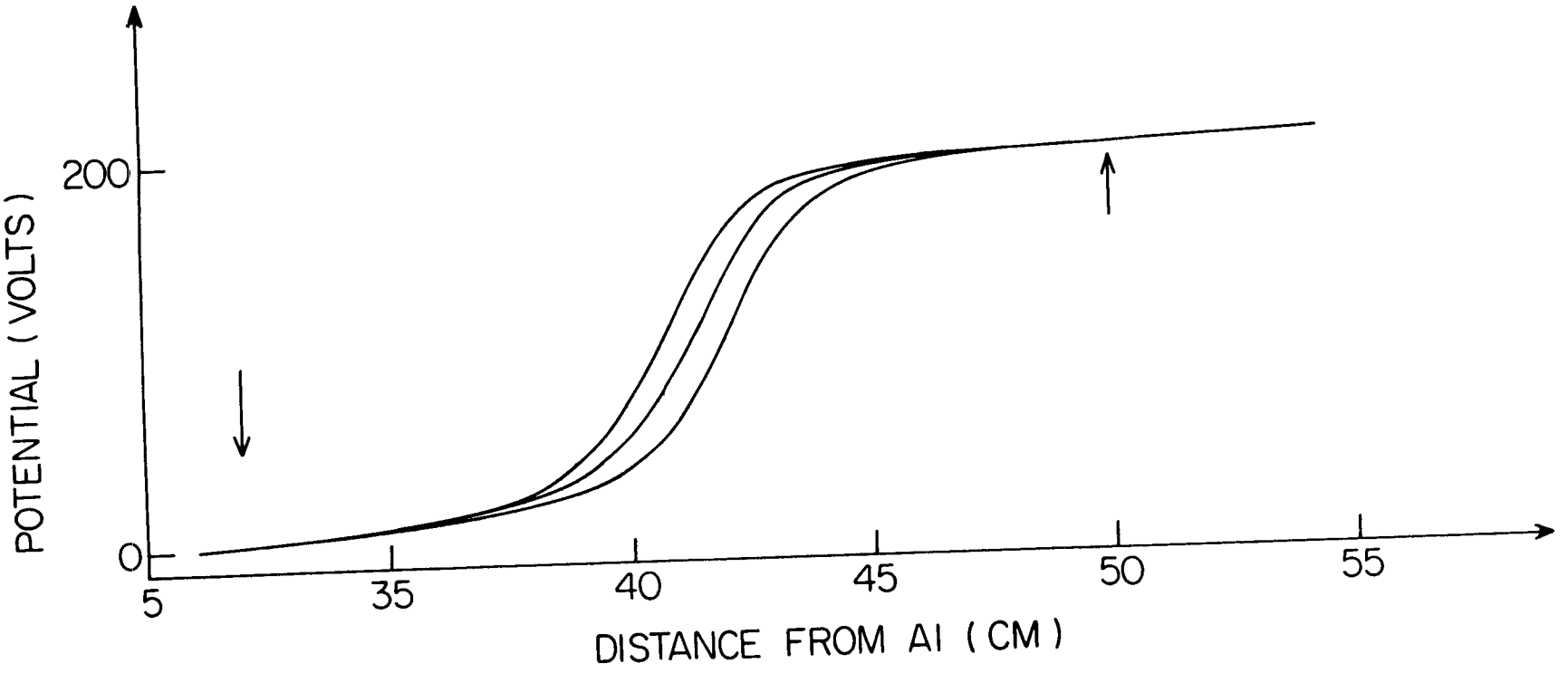

Figure 8. Potential structures obtained using a fixed probe to provide a gate, when the potential reached certain preset values, for the signal from the moving probe. Results for three different trigger levels are shown.

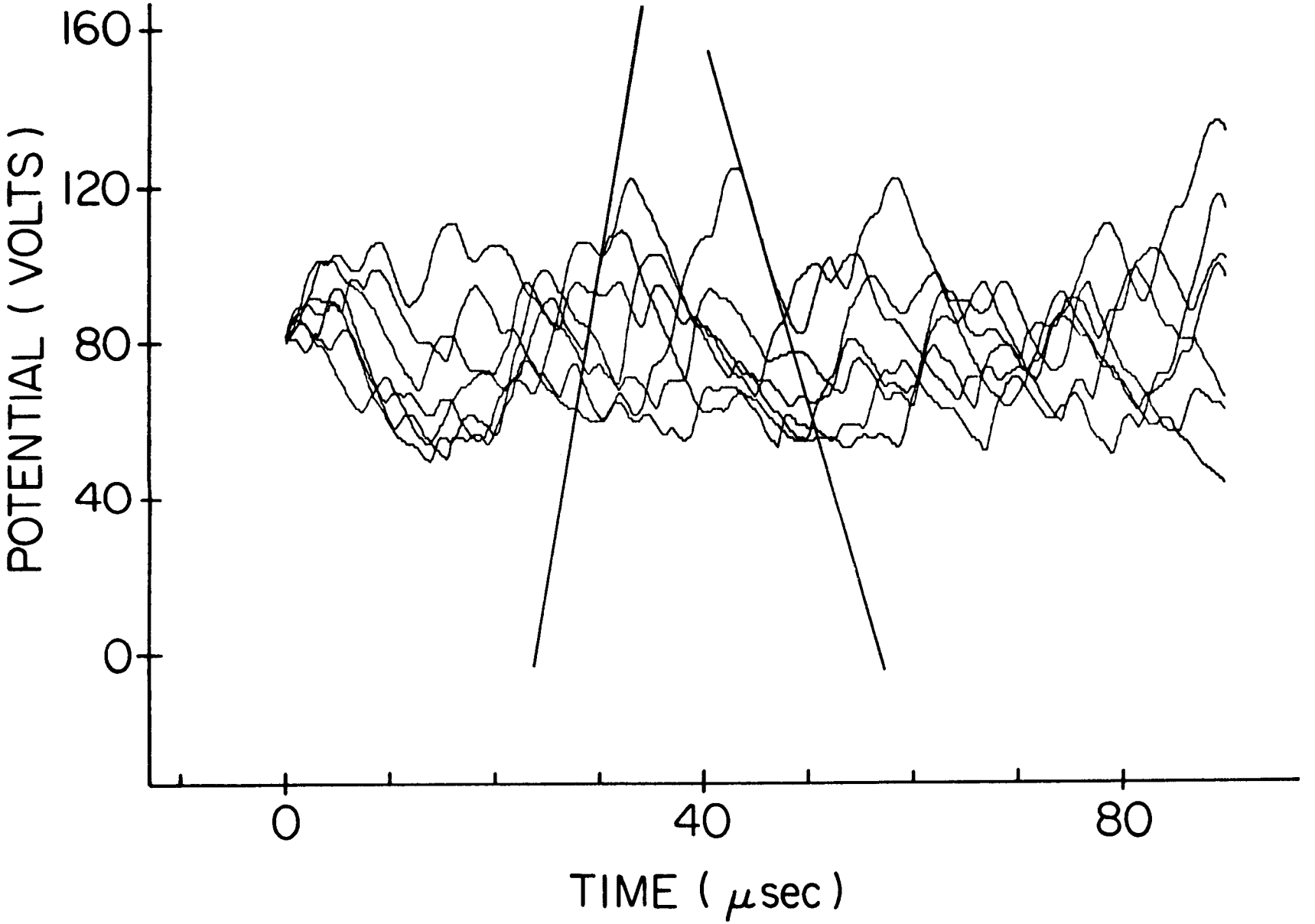

Figure 9. Oscilloscope traces similar to those shown in Figure 8 but taken with a probe with greatly reduced distributed capacitance.

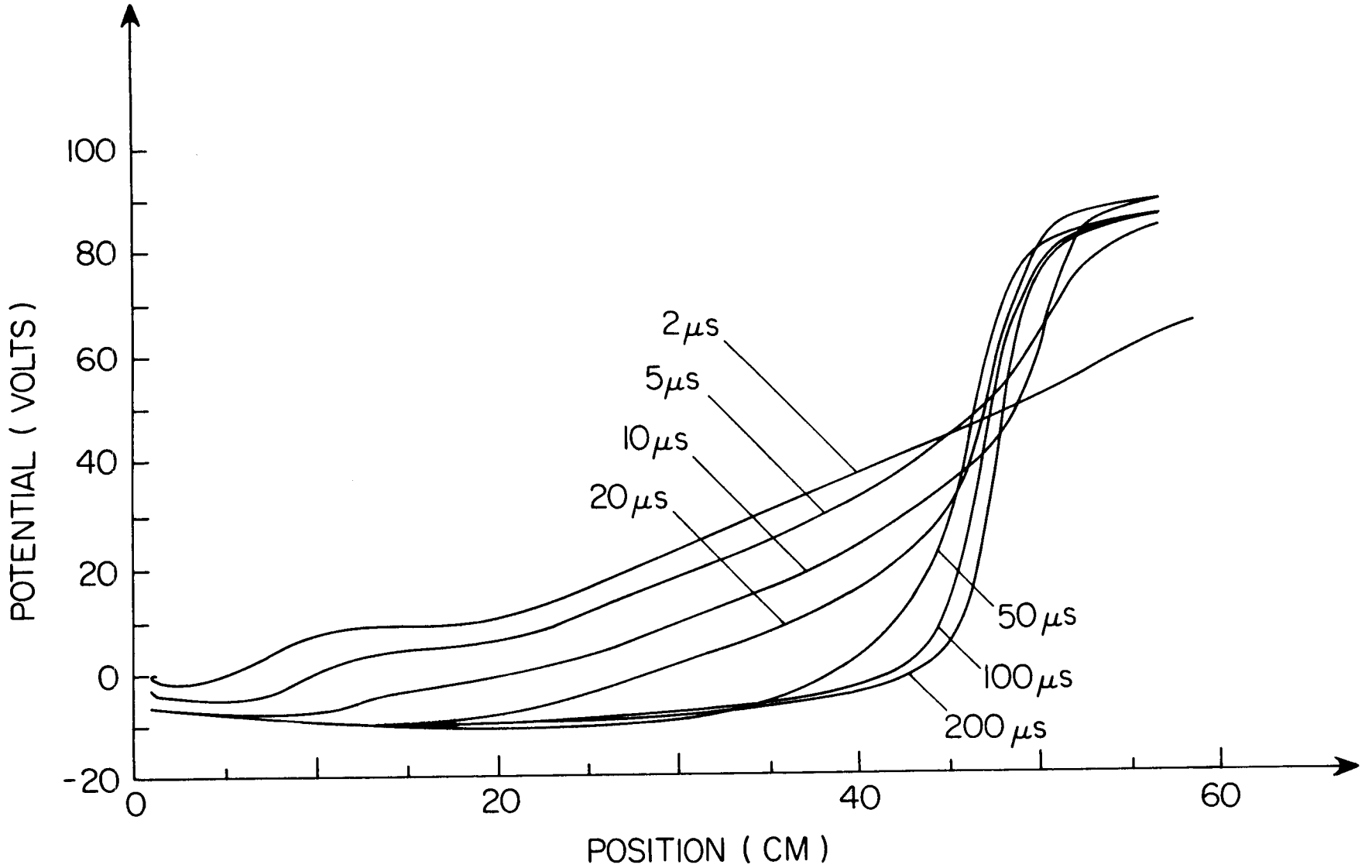

Figure 10. Measured potential structure at various times after the high voltage was switched on. The double layer forms quickly from an initial state where the structure is nearly that of a vacuum capacitor.